3D modeling of the flow and heat transfer during DC casting with a combo bag

Ilinca, Florin; Hétu, Jean-Francois; Arsenault, André; Larouche, Daniel; Tremblay, Sylvain P.

3D MODELING OF THE FLOW AND HEAT TRANSFER DURING DC CASTING WITH A COMBO BAG

Florin Ilinca[1], Jean-François Hétu[1], André Arsenault[2], Daniel Larouche[2], Sylvain P. Tremblay[3]
[1]Industrial Materials Institute, NRC; 75 de Mortagne; Boucherville, QC, J4B 6Y4, Canada
[2]Laval University, Dept. of Mining, Metal. and Mat. Eng., Adrien-Pouliot Bldg, Québec, QC, G1K 7P4, Canada
[3]PYROTEK INC., 1623 Manic Street, Saguenay, QC, G7K 1G8, Canada

Keywords: Aluminum casting, Combo bag, Fluid modeling, Heat transfer

Abstract

The goal of this study is to determine the influence of combo bag on the velocity and temperature fields in the liquid metal pool during the DC casting of aluminum ingots. For this, a 3D finite element solution algorithm is used to compute the flow and heat transfer phenomena. The solution approach is able to deal with high Reynolds number turbulent flows, buoyancy effects and flow through combo bag meshed openings. An isothermal study with turbulence modeling quantifies the effect of the combo bag on the flow and an effective viscosity is determined for the respective flow conditions. The coupled flow and heat transfer during ingot formation are solved for forced convection conditions (no buoyancy) and by including the natural convection terms. It is shown that the flow is driven by the inlet flow rate in the vicinity of the combo bag and by natural convection outside this region.

Introduction

The distribution of liquid metal in DC casting pits receives a lot of attention in the past by process engineers, operators and suppliers. Most efforts to improve the performance of these systems were made by trials and errors giving rapid solutions for today, but few insights helping the development of the next generation of systems components. The mass flow of metal is relatively easy to calculate from the holding furnace to the dip tube but the situation becomes very complex when the metal flows down in the distribution bag and later on in the sump of the cast ingot. Unfortunately, this is exactly where it would be interesting to have an accurate description of the flow of metal since the recirculation loops inside the sump have surely an impact on the cooling conditions prevailing at the periphery of the sump. To which extent this phenomenon is dominant is still unknown.

Last year, Arsenault and co-workers [1] presented a 3D thermal – fluid flow simulation of ingot DC casting using a semi-permeable model of a Thermally Formed (TF) combo bag. This model was developed to simulate the effects produce by the full coupling between the flow in the dip tube, in the combo bag and in the sump. Due to the limitations of the machine used to solve the conservative equations it was not possible to obtain a true stationary solution and to verify the influence of turbulence. This model was imported in another platform, allowing much smaller computation time and giving us the opportunity to verify the influence of turbulence. This paper presents new results and observations obtained with this platform.

Model Equations

The CFD model solves differential equations describing the conservation of mass, momentum and energy in order to evaluate the velocity, pressure and temperature fields. The flow is driven by the incompressible Reynolds Averaged Navier-Stokes equations:

$$\rho\left(\frac{\partial \mathbf{u}}{\partial t}+\mathbf{u}\cdot\nabla\mathbf{u}\right)=-\nabla p+\nabla\cdot[2(\mu+\mu_T)\dot{\gamma}(\mathbf{u})]+\rho\mathbf{g}\beta\left(T-T_0\right)+\mathbf{f} \quad (1)$$

$$\nabla\cdot\mathbf{u}=0 \quad (2)$$

where $\dot{\gamma}(\mathbf{u})=(\nabla\mathbf{u}+\nabla\mathbf{u}^T)/2$ is the strain rate tensor. The heat transfer is modeled by the energy equation:

$$\rho\left(\frac{\partial h}{\partial t}+\mathbf{u}\cdot\nabla h\right)=\nabla\cdot\left[\lambda\cdot\nabla T\right] \quad (3)$$

In the above equations, t, $\mathbf{u}$, p, T, ρ, μ, h and λ denote time, velocity, pressure, temperature, density, viscosity, mass enthalpy and thermal conductivity respectively. In the momentum equation $\mathbf{f}$ denotes an external source term and the buoyancy is modeled through the Boussinesq approximation depending on the reference density (the density estimated at the reference temperature T_0), gravity vector $\mathbf{g}$, thermal expansion coefficient β, and the temperature difference between that of the liquid aluminum and the reference value T_0 [2].

The turbulent eddy viscosity μ_T is computed using the standard $\kappa-\varepsilon$ model of turbulence:

$$\mu_T=\rho C_\mu\frac{\kappa^2}{\varepsilon} \quad (4)$$

For this model, the turbulence quantities are the turbulence kinetic energy κ and its dissipation rate ε. The transport equations for κ and ε are [3]:

$$\rho\left(\frac{\partial \kappa}{\partial t}+\mathbf{u}\cdot\nabla\kappa\right)=\nabla\cdot\left[\left(\mu+\frac{\mu_T}{\sigma_k}\right)\nabla\kappa\right]+\mu_T P(\mathbf{u})-\rho\varepsilon \quad (5)$$

$$\rho\left(\frac{\partial \varepsilon}{\partial t}+\mathbf{u}\cdot\nabla\varepsilon\right)=\nabla\cdot\left[\left(\mu+\frac{\mu_T}{\sigma_\varepsilon}\right)\nabla\varepsilon\right]+C_{\varepsilon 1}\frac{\varepsilon}{\kappa}\mu_T P(\mathbf{u})-C_{\varepsilon 2}\rho\frac{\varepsilon^2}{\kappa} \quad (6)$$

where the production of turbulence is $P(\mathbf{u})=\nabla\mathbf{u}:\left(\nabla\mathbf{u}+\nabla\mathbf{u}^T\right)$. The model constants are as follow: $\sigma_k=1.0$, $\sigma_\varepsilon=1.3$, $C_{\varepsilon 1}=1.44$, $C_{\varepsilon 2}=1.92$, $C_\mu=0.09$.

Boundary conditions for the momentum equations are specified on the metal inlet plane and on solid boundaries (walls) as follows:

$$\begin{aligned} \mathbf{u}&=U_i && \text{on the inlet}\\ \mathbf{u}&=0 && \text{at the walls}\\ 2(\mu+\mu_T)\dot{\gamma}(\mathbf{u})\cdot n-pn&=0 && \text{on the free surface}\end{aligned} \quad (7)$$

Model Description

The geometry of the model is basically the same as the one presented in [1]. The computational domain was discretized using 4-node tetrahedral finite elements. The mesh for the isothermal

flow case (no sump) has 141,971 nodes and 759,772 elements, whereas the one used for the thermal model has 148,161 nodes and 846,839 elements. Figure 1 illustrates the finite element discretization for the isothermal flow case.

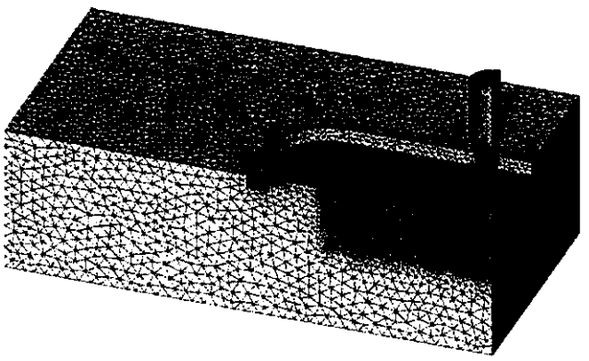

Figure 1: Geometry and meshing of the model

Boundary conditions

The inlet velocity was imposed on the cross section defining the entry plane of liquid metal. The casting speed is 50.8 mm/min and the corresponding inlet velocity conserving the volumetric flow is 240 mm/s. Non-slip boundary conditions were imposed on solid walls, whereas the liquid top surface was constrained to remain horizontal by imposing the vertical velocity to zero.

The inlet temperature is set to 700°C and convective heat boundary conditions were applied on the external walls of the ingot and on the liquid metal distribution system [1]. The convective heat transfer coefficient and ambient temperature were set to (HTC=10 W/m^2/K, T_∞=20°C) for the upper part of the model. Side cooling of the ingot was divided in three zones: 1) the primary cooling zone (57 mm long) representing the heat extracted by the mold for which (HTC=500 W/m^2/K, T_∞=100°C); 2) the air gap (25.4 mm long) representing a small zone without water cooling (HTC=10 W/m^2/K, T_∞=20°C), and 3) the secondary cooling zone representing the sides exposed to water cooling (HTC=10,000 W/m^2/K, T_∞=25°C) [4]. A convective boundary condition was also imposed at the bottom of the ingot to simulate the axial heat extraction (HTC=500 W/m^2/K, T_∞=25°C).

Material properties

The material properties were considered as from the work of Arsenault et al. [1]. Polynomial formulas were developed for the solid fraction which then was used to compute the density, specific heat and thermal conductivity. The solid fraction is computed as from:

$$f_s = 1, \text{ for } \tilde{T} \le 0$$
$$f_s = a\tilde{T}^3 + b\tilde{T}^2 + c\tilde{T} + d, \text{ for } 0 \le \tilde{T} \le 1 \quad (8)$$
$$f_s = 0, \text{ for } 1 \le \tilde{T}$$

with $\tilde{T} = (T - T_s)/(T_l - T_s)$. The constants take on the values $T_s = 620.25^0C$, $T_l = 648.86^0C$, $a = -0.7795$, $b = 0.2716$, $c = -0.4921$ and $d = 1$.

The density is given by:

$$\rho = \rho_0 + C_T(T - T_0) + C_{f_s}(1 - f_s) \quad (9)$$

where $C_T = -0.305 kg/(m^3 \cdot K)$, $C_{f_s} = -145 kg/m^3$, $T_0 = 556^0C$ and $\rho_0 = 2546.15 kg/m^3$.

The mass enthalpy is given by:

$$h = h_0 + C_{p0}(T - T_0) + L(1 - f_s) \quad (10)$$

where $L = 389 kJ/kg$, $h_0 = 547 kJ/kg$, $C_{p0} = 1070 J/(kg \cdot {}^0C)$.

The thermal conductivity is given by:

$$\lambda = \lambda_0 + C_k(1 - f_s) \quad (11)$$

where $\lambda_0 = 180547 W/(m \cdot K)$ and $C_k = -93 W/(m \cdot K)$.

Solution algorithm

The global system of equations is solved in a partly segregated manner. At each time step global iterations are performed for the momentum-continuity, turbulence and energy equations. Turbulence equations are solved for the logarithm of turbulence variables. Sub-iterations of turbulence transport equations are also used to accelerate the overall convergence of the iterative process [3]. For the isothermal case, the steady state solution is obtained from the iterative solution of the momentum-continuity and turbulence equation. For the thermal problem with buoyancy, the transient solution is obtained during a time frame of 15 min by using as initial solution the temperature distribution given by a heat transfer problem with the velocity given by the descent velocity of the ingot.

The Navier-Stokes and scalar transport equations are solved using a Streamline-Upwind Petrov-Galerkin (SUPG) method. This method contains additional stabilization terms providing smooth solutions to convection dominating flows. The SUPG method also deals with velocity-pressure coupling so that equal-order interpolation results in a stable numerical scheme. This allows the use of simple linear elements for all variables.

Computations were performed in parallel on a 64-node Beowulf cluster. Each node consists of an Intel motherboard with two Intel Xeon 3.4Ghz (FSB-800) and 2GB of RAM. Computational nodes are connected with Myrinet 2000 (PCIXD) cards and switches and MPICH-GM is used.

Process Modeling

Modeling the flow through the fabric cloth

The fabric cloth considered has the same characteristic than the one described in reference [1]. To determine the pressure drop through the fabric cloth a single cell unit was considered and the flow domain was meshed with 3D tetrahedral elements. The mesh is sufficiently refined in order to capture well the flow and contains 374,000 elements and 79,596 nodes.

Several computations were carried out for velocities ranging from 0.002m/s to 0.256m/s. It was observed that for the highest velocities the flow becomes unstable indicating that turbulence may occur. Hence, two series of computations were carried out, one for the laminar regime and a second one using the κ-ε turbulence model. The results for the pressure drop are shown with symbols (squares for the laminar solution and circles for the turbulent solution) in Figure 2.

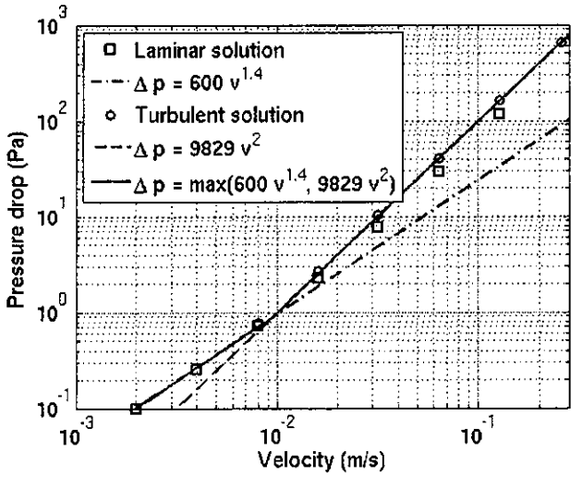

Figure 2: Pressure drop through the fabric cloth

It was observed that the pressure drop varies as $600v^{1.4}$ for the lower velocities and then as $9829v^2$ at larger velocity. For velocities larger than 0.256m/s the pressure drop remains proportional with the square of the velocity. A good model describing the pressure drop through the fabric cloth as a function of the velocity is therefore given by:

$$\Delta p = \max(600v^{1.4}, 9829v^2) \tag{12}$$

This pressure drop would be modeled using a source term in the momentum equations:

$$\mathbf{f} = -\frac{\Delta p}{\delta}\frac{\mathbf{v}}{|\mathbf{v}|} \tag{13}$$

where δ is the thickness of the fabric cloth layer.

Isothermal flow through the combo bag

A first computational configuration is used to validate the flow in the combo bag. The model does not consider the ingot and therefore it can be considered isothermal. Simulations were carried out for steady state conditions and an inlet velocity of 240 mm/s. The flow is highly convective and therefore a time marching scheme was used to obtain the steady state solution. The Reynolds number based on the conditions in the inlet channel is Re=56,800 indicating that the flow is turbulent. The observed velocity in the fabric cloth region is smaller than 50 mm/s. At this flow rate, the laminar and turbulent flow solutions through the fabric cloth give similar pressure drop (Figure 2).

In order to assess the effect of the viscosity and of the turbulence model on the flow solution, simulations were carried out for the laminar flow conditions at viscosities equal to the nominal value ($1.15 \cdot 10^{-3} Pa \cdot s$), 10 times larger and 100 times larger and for the turbulent flow conditions using the κ-ε turbulence model. The solutions are compared in Figure 3 which shows the regions of the flow were the velocity is higher than 100 cm/min. The colors are as from the velocity magnitude, with the red indicating velocities higher than 500 cm/min.

As can be seen, the laminar flow solutions at the nominal viscosity and for the 10 times higher viscosity are comparable. The flow is highly convective and a strong jet develops from the region inside the impervious skirt. Flow of smaller intensity is observed through the fabric cloth at the bottom of the combo bag. The solution for a viscosity 100 times higher than the laminar viscosity seems to be over diffusive, as the jet of material from the impervious skirt is of much smaller intensity. This indicates that solving the laminar flow conditions with this value of the viscosity would be too diffusive. Finally, the solution was also obtained for the turbulent flow conditions using the κ–ε turbulence model. We should mention in this case that given the way in which the fabric cloth was modeled (as an equivalent porous material), neglecting the actual geometry and boundary of the fabric cloth, the turbulence generation in the region of the fabric cloth is neglected. The turbulent flow solution also presents an important jet of material from inside the impervious skirt, but having smaller amplitude than observed for the laminar flow solution. Finally, it was found that the laminar flow solution for an effective viscosity 40 times the laminar viscosity gives results comparable to those for turbulent flow computation (see Figure 4 and 3-d). This effective viscosity was considered in the work presented in the following section.

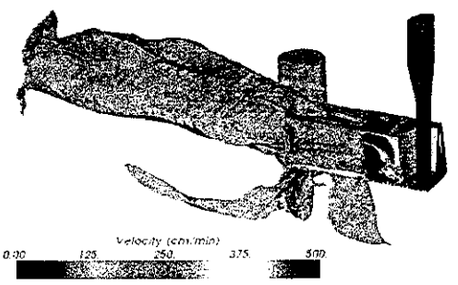

(a) Laminar viscosity

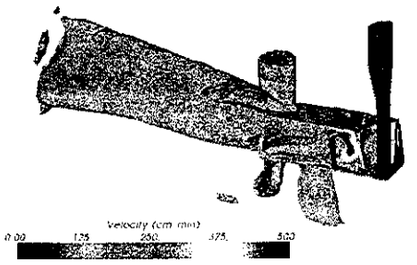

(b) Laminar 10x(viscosity)

(c) Laminar 100x(viscosity)

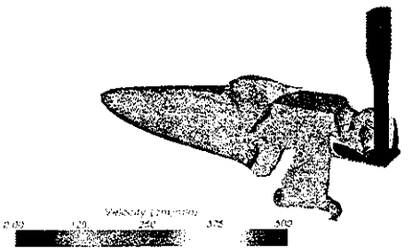

(d) Turbulent, κ–ε model

Figure 3: Region of velocity higher than 100cm/min

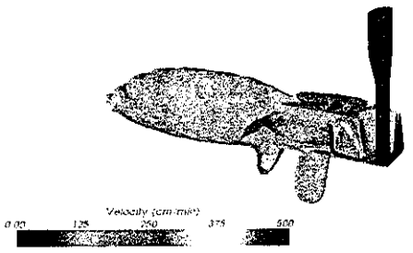

Laminar $\mu_{eff} = 40\mu$

Figure 4: Effective viscosity laminar flow

Thermal flow solution with ingot

The thermal flow computations were carried out starting with an initial temperature distribution obtained from a no flow computation (the velocity is imposed as from the ingot velocity). The heat transfer coefficient in the water cooled region is $h = 10000W/(m^2 \cdot K)$ [4], whereas on the remaining surfaces the same conditions as described in [1] were considered. The thermal expansion coefficient was first considered as given by the density-temperature dependence ($\beta = 128 \cdot 10^{-6} K^{-1}$) and then a second run was performed without the presence of the natural convection term (forced convection with $\beta = 0$). The solution for the temperature during the first 6 seconds of simulation is compared with the initial temperature in Figure 5 for the case that includes the natural convection term. It can be seen that the temperature varies very rapidly and the flow produces a more uniform temperature in the liquid pool above the solid ingot. The region of higher temperature decreases as the liquid metal with higher temperature has lower density and tends to flow towards the top free surface. The position of the liquid / solid interface does not change during the first 6 seconds of simulation. The temperature at later times is shown in Figure 6 which shows that the temperature changes little after the first 20 seconds of simulation. The higher temperature metal from the inlet flows towards the top surface and the temperature is more uniform at a level closer to the liquidus temperature of 649°C in the liquid region below. In order to estimate the influence of the natural convection term on the flow and temperature distribution, a second simulation was carried out without the presence of the natural convection term. The temperature field for this case is shown in Figure 7. Significantly different temperature distributions are observed. In this case, the higher temperature material is pushed outside the bag laterally and towards the bottom as previously observed in the isothermal test case. The temperature distribution changes gradually with time and the high temperature region is larger than in the previous case. Remark that the Boussinesq term determines an important natural convection flow in regions having high temperature gradient. In the present case the Boussinesq term becomes dominant in the region outside the combo bag and determines a stratified temperature field. The high temperature material having a lower density naturally flows toward the top surface, whereas the lower temperature material flows to the bottom of the liquid pool. The velocity scale of the flow induced by the temperature gradient is given by:

$$U_s = \sqrt{Lg\beta\Delta T} \tag{14}$$

For the characteristic values L=80mm, g=10m/s^2, $\beta = 128 \cdot 10^{-6} K^{-1}$, $\Delta T = 10K$ we obtain that the velocities induced by the Archimedes forces are of the order of 200 cm/min. This value is comparable with the velocity in the jets from the combo bag. It also indicates that outside a region close to the combo bag the flow is mostly driven by the natural convection.

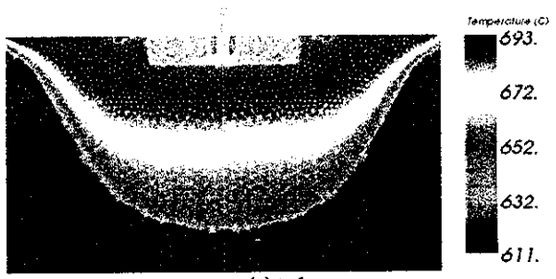

(a) t=1s

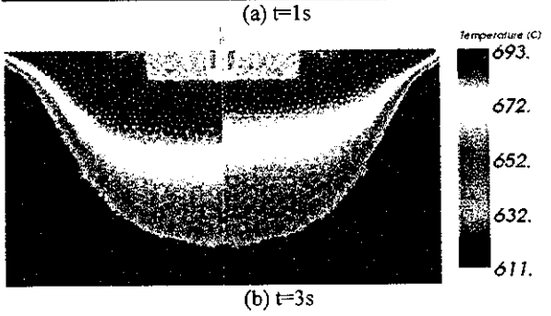

(b) t=3s

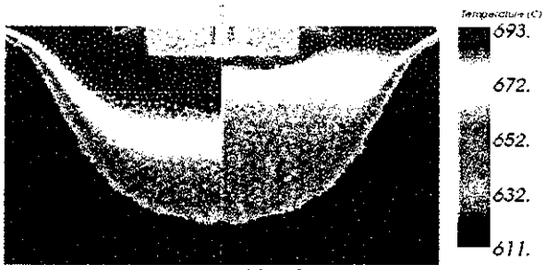

(c) t=6s

Figure 5: Initial temperature distribution compared with the solution for t=1s to t=6s for natural convection solution

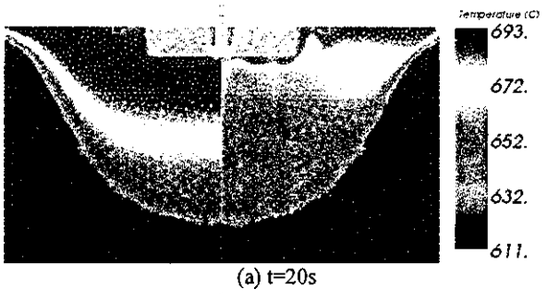

(a) t=20s

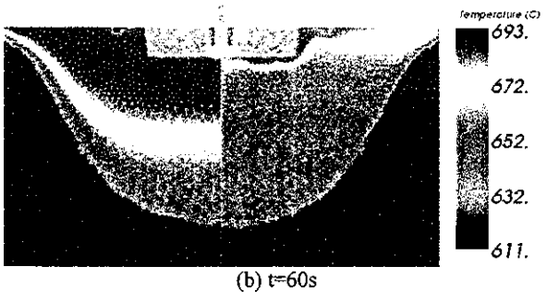

(b) t=60s

Figure 6: Initial temperature distribution compared with the solution at t=20s and t=60s for natural convection solution

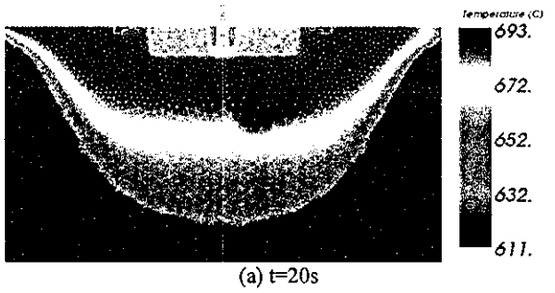

(a) t=20s

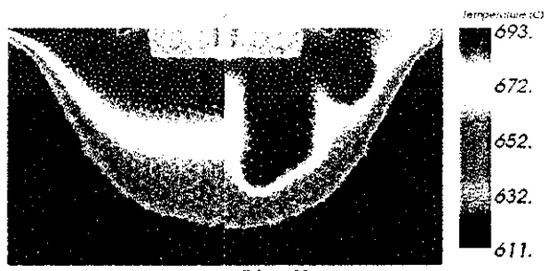

(b) t=60s

Figure 7: Initial temperature distribution compared with the solution at various times for forced convection solution (no Boussinesq term)

The velocity distribution for the solution with natural convection at t=10s is illustrated in Figure 8, Figure 9 and Figure 10. Figure 8 shows the velocity distribution in planes parallel to the longer side of the ingot. The flow is shown in the symmetry plane (Z=0) and at 25mm from the symmetry plane. As can be seen, the effect of the flow from the combo bag is limited to a narrow region around the combo bag. Outside this region the flow is driven by the natural convection. The effect of the Boussinesq term is that the colder material near the liquid / solid interface flows to the bottom of the sump (because has higher density). To compensate for this flow, the material near the center of the bath flows towards the top surface. The natural convection flow in this region generates a more uniform temperature. A similar flow is observed in planes parallel to the shorter side of the ingot (Figure 9). Here again we observe that except for the region close to the combo bag, the flow is driven by the natural convection term. The flow exchange is also illustrated in Figure 10, where the velocity in shown in a horizontal plane. Again we observe that the flow is downward in the region close to the liquid / solid interface and upward near the center of the domain were the temperature is higher.

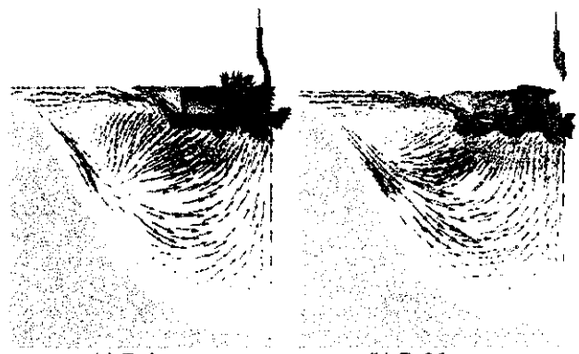

(a) Z=0 (b) Z=25mm

Figure 8: Velocity distribution in planes parallel to the XY plane

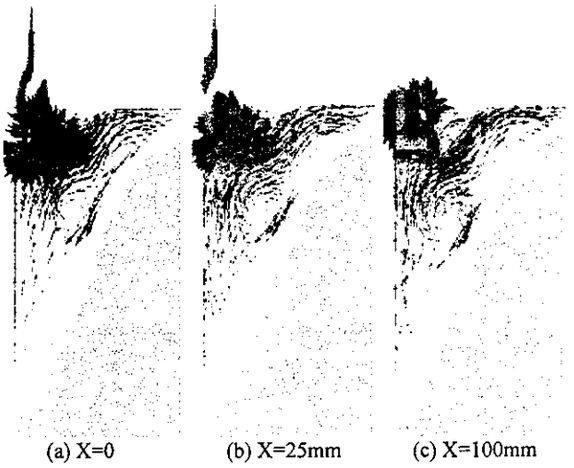

Figure 9: Velocity distribution in planes parallel to the YZ plane

Figure 10: Velocity distribution in a plane parallel to the XZ plane

Analysis of Numerical Results

The results indicate that the flow outside the combo bag is driven by natural convection. The temperature in the liquid pool on top of the ingot is more uniform when considering the effect of natural convection and the material with higher temperature flows towards the top surface.

The following conclusions can be drawn from the numerical results obtained:

- The flow through the fabric cloth can be effectively modeled by using a porous media approach. In the present case this was taken into account by the addition of a source term that produces the same pressure drop as the fabric cloth.
- The isothermal flow in the combo bag shows that an important jet develops along the longer side of the basket. This is in agreement with the experimental observations on a water model. A second jet is observed below the basket and oriented towards the bottom of the computational domain.
- The initial temperature was obtained from a cooling computation with the velocity imposed as given by the ingot descend velocity. This temperature distribution agrees well with the one computed by ProCast [1].
- The flow and temperature distributions for the complete case indicate an important natural convection contribution in the region below the combo bag. The temperature is relatively uniform in this region. The high temperature liquid metal flows towards the top surface, whereas the flow in the region below the basket is driven by the natural convection. The lower temperature metal near the liquid / solid interface flows to the bottom and the liquid near the center of the domain flows upward. This mixing determines a more uniform temperature in this region.

Conclusions

The present work allowed us to study the intensity of two important phenomena occurring in the liquid metal pool during DC casting. First, the turbulence intensity level was gauged against the forced convective flow area at the exit of the metal distributor. The shape and force of the liquid metal jets were used to determine an appropriate equivalent turbulent viscosity. Second, the impact of natural convection on the contour-plot of isotherms in the liquid metal pool has been illustrated. The drastic change in isotherm pattern when the natural convection model is activated indicates that natural convective flow is at least as important as the forced convective flow to drive the recirculation loops.

Despite the importance of natural convection in the development of the stationary temperature distribution below the combo bag, the forced convective flow produce by the combo bag still exerts an important influence in the upper portion of the pool, where solidification starts and defects are most likely to occur. Future works will then essentially focus on the quantification of the impact of combo bags on the heat transfer occurring at the periphery of the upper portion of the sump.

Acknowledgements

The authors express their gratitude to the Centre Québécois de recherche et de développement de l'aluminium for its financial support.

References

[1] A. Arsenault, D. Larouche, S.P. Tremblay, J.P. Dubé, "DC cast thermal and fluid flow simulation using a semi-permeable model of TF combo bag," Light Metals 2008, D.H. DeYoung, ed., The Minerals, Metals & Materials Society, 2008, pp. 781-785.

[2] F. Ilinca, J.-F. Hétu, "Three-dimensional numerical simulation of turbulent flow and heat transfer in a continuous galvanizing bath," Num. Heat Tranfer, Part A, vol. 44, 2003, pp. 463-482.

[3] F. Ilinca, J.-F. Hétu, "Finite Element Solution of Three-Dimensional Turbulent Flows Applied to Mold-Filling Problems," Int. J. for Numerical Methods in Fluids, vol. 34, 2000; pp.729-750.

[4] A.J. Williams, T.N. Croft and M. Cross, "Modeling of Ingot Development during the Start-Up Phase of Direct Chill Casting", *Met. Mater. Trans.*, Vol. 34B, 2003, pp. 727-734.